Physics Letters B 773 (2017) 159–165

Contents lists available at ScienceDirect

Physics Letters B

www.elsevier.com/locate/physletb

Can nuclear physics explain the anomaly observed in the internal pair production in the Beryllium-8 nucleus?

Xilin Zhang *, Gerald A. Miller

Department of Physics, University of Washington, Seattle, WA 98195, USA

ARTICLE INFO

Article history:
Received 29 March 2017
Received in revised form 7 August 2017
Accepted 8 August 2017
Available online 16 August 2017
Editor: W. Haxton

ABSTRACT

Recently the experimentalists in Krasznahorkay (2016) [1] announced observing an unexpected enhancement of the e^+–e^- pair production signal in one of the ^{8}Be nuclear transitions. The subsequent studies have been focused on possible explanations based on introducing new types of particle. In this work, we improve the nuclear physics modeling of the reaction by studying the pair emission anisotropy and the interferences between different multipoles in an effective field theory inspired framework, and examine their possible relevance to the anomaly. The connection between the previously measured on-shell photon production and the pair production in the same nuclear transitions is established. These improvements, absent in the original experimental analysis, should be included in extracting new particle's properties from the experiment of this type. However, the improvements can not explain the anomaly. We then explore the nuclear transition form factor as a possible origin of the anomaly, and find the required form factor to be unrealistic for the ^{8}Be nucleus. The reduction of the anomaly's significance by simply rescaling our predicted event count is also investigated.

1. Introduction

It was announced in Ref. [1] that in the measurement of the e^+–e^- pair production in the ^{8}Be's nuclear transition between one of its 1^+ resonance and its ground state (GS, a narrow resonance), an unexpected enhancement of the signal was observed in the large e^+–e^- invariant mass region (about 17 MeV) and in the large pair correlation angle (near 140°) region. The observation has generated strong interest in the particle physics community, because the anomaly could be explained by new types of particles (e.g., [1,2]). However, the nuclear physics model from Ref. [3] as used by the experimentalists for simulating the pair production [4] through virtual photon decay is incomplete. In the experiment, the initial state is a beam-target plane wave and sets up a particular direction in the reaction, leading to anisotropy in the pair emission. Moreover, in the anomalous reaction channel, the E1 and M1 multipoles have similar weights and their interference is substantial. Furthermore, the on-shell photon production measurements [5–9] provide important constraints on the multipoles in the pair production. In this work, we set up a model inspired by the so-called Halo effective field theory (EFT) framework [10,11], taking into account the aforementioned factors which have not been addressed before [3], calibrate it to the photon production data, and predict the pair production cross section. The results, as well as the approach, could be used for analyzing future experiment of this type. Although a direct comparison to the current e^+–e^- data is not feasible due to the missing public information about the experimental detector efficiency [4], the shape comparisons are still valuable. We find that the model improvements are not able to explain the anomaly. We also evade the photon production constraint by invoking a hypothetical form factor for the M1 transition, and show that the form factor needed to explain the anomaly suggests an unrealistic large length scale on the order of 10s fm for the ^{8}Be nucleus. We then study how the anomaly's significance is modified when the normalizations of our event estimation are allowed to vary. In the following, section 2 discusses the kinematics and our model; section 3 is about the model calibration. We then present our pair-production results in section 4, and explore possible M1 transition form factor in section 5. A short summary is provided in the end.

2. Kinematics and the EFT-inspired model

Fig. 1 illustrates the relevant kinematic variables for both pair and photon productions in the proton–^{7}Li CM frame. $\boldsymbol{p}$, $\boldsymbol{p}_+$, and

* Corresponding author.
E-mail addresses: xilinz@uw.edu (X. Zhang), miller@phys.washington.edu (G.A. Miller).

http://dx.doi.org/10.1016/j.physletb.2017.08.013

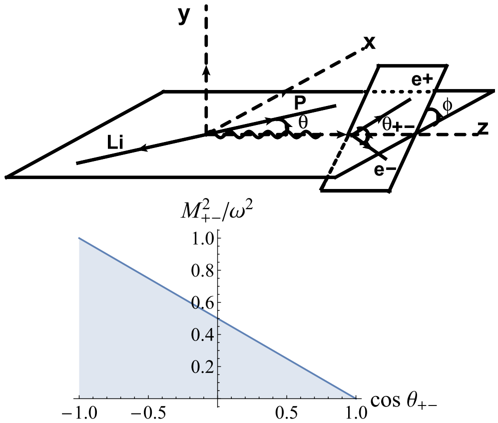

Fig. 1. The top shows the kinematics for the e^+–e^- pair production as well as the photon production (without the lepton line). The bottom plots the allowed phase space (shaded area) in terms of M_{+-} and $\cos\theta_{+-}$ assuming $m_e = 0$.

$\boldsymbol{p}_-$ are the proton–^{7}Li relative momentum and the momenta of e^+ and e^-. Given $|\boldsymbol{p}|$, there is one degrees of freedom (DOF), θ, in the photon production, and four in the pair production: θ, θ_{+-}, ϕ, and positron energy E_+ [electron energy $E_- = \omega - E_+$ with ω being the (virtual) photon's energy]. The total pair production cross section can then be computed through [3]:

$$\sigma_{e^+e^-} = \frac{M}{p}\frac{\alpha}{16\pi^3}\int dE_+ d\cos\theta_{+-}\, d\cos\theta\, d\phi \times \frac{p_+ p_-}{8}\sum_{\text{spins}} |\mathcal{M}_{e^+e^-}|^2 \,. \tag{2.1}$$

Since the original experimental report [1] shows data vs. θ_{+-} and the pair's invariant mass $M_{+-} \equiv \sqrt{\omega^2 - (\boldsymbol{p}_+ + \boldsymbol{p}_-)^2}$ separately, formula for computing $d\sigma$ vs. dM_{+-} and $d\theta_{+-}$ are needed. To calculate $d\sigma/dM_{+-}$ based on Eq. (2.1), the relation, $p_+ p_- dE_+ d\cos\theta_{+-} = q p'_+ dM_{+-} d\cos\theta'_+$, could be used; the "primed" variables are measured in the e^+–e^- CM frame, e.g., $p'_+ = p'_- = \sqrt{M_{+-}^2/4 - m_e^2}$ with m_e as the electron mass. In the phase space where $\cos\theta_{+-} < 0$ and $E_+, E_- \gg m_e$, $m_e = 0$ approximation can be applied to simplify the relationship between E_+ and M_{+-} at fixed θ_{+-}: $dE_+/dM_{+-} = M_{+-}/[\omega|y|(1-\cos\theta_{+-})]$ with $y \equiv (E_+ - E_-)/\omega$, which is then used to compute $d\sigma/dM_{+-} d\cos\theta_{+-}$ based on Eq. (2.1). The allowed phase space is shown in the bottom panel of Fig. 1: given a negative $\cos\theta_{+-}$, $4m_e^2 \le M_{+-}^2 \le \omega^2(1-\cos\theta_{+-})/2$. We can see that the large-M_{+-} events have large θ_{+-}, while the large-θ_{+-} events have M_{+-} from $4m_e^2$ to its upper bound and part of the Jacobian factor, $M_{+-}p_+p_-/|y|$, enhances the contribution from the large M_{+-} region. Although Ref. [1] shows that the anomaly exists in the large M_{+-} (θ_{+-}) region of $d\sigma/dM_{+-}$ ($d\sigma/d\cos\theta_{+-}$) distribution, it should be informative to see where the anomaly resides in the joint (M_{+-}, θ_{+-}) phase space. Note for a fixed y, $M_{+-}^2 = (1-y^2)\omega^2(1-\cos\theta_{+-})/2$, which corresponds to a straight line in the phase space intersecting the horizontal axis at $\cos\theta_{+-} = 1$, e.g., the solid curve ($y = 0$) in the plotted phase space.

The key quantity in modeling is the EM current's matrix element, $\langle \text{Be8}; -\boldsymbol{q}|\hat{J}^\mu(\boldsymbol{q})|\text{Li7} + \text{p}; a, \sigma, \boldsymbol{p}\rangle$ with a and σ as ^{7}Li and proton spin projections and $\boldsymbol{q}$ as the (virtual) photon momentum. The matrix element has different components, denoted as $U_{\lambda SL}$ with λ, S, and L labeling virtual photon's multipolarity, initial state's total spin and orbital angular momentum. In the J^π notation, ^{7}Li, proton, ^{8}Be GS, and its excited states of interest are $\frac{3}{2}^-$, $\frac{1}{2}^+$, 0^+, and two 1^+s [5,12]. As dictated by the parity conservation and Wigner–Eckart theorem, the E1 transition is between the s-wave ($L = 0$) proton–^{7}Li scattering state and the ^{8}Be GS (d-wave should be small), and the total spin S can only be 1; for the M1 transition $L = 1$ and $S = 1$ or 2. The role of E2 transition is also explored here, whose $L = 1$ and $S = 1$ or 2. In total, five amplitudes need to be addressed, U_{110} for E1, U_{111} and U_{121} for M1, U_{211} and U_{221} for E2.

It is worthwhile to mention a few momentum (length) scales in the reactions. The ^{7}Li GS is 2.467 MeV below its breakup threshold—to ^{4}He+^{3}H [12]—which translates to a binding momentum $\Lambda \approx 10^2$ MeV if ^{7}Li is considered as the bound state of the fragments; the corresponding length scale is 2 fm. Meanwhile, the ^{8}Be's *mostly* iso-scalar (MIS) and iso-vector (MIV) 1^+ resonances are $E_{(0)} = 0.895$ and $E_{(1)} = 0.385$ MeV above the proton–^{7}Li threshold (as measured in the proton–^{7}Li CM frame) [5]; the associated momenta p are about 40 and 25 MeV (5 and 8 fm in length scale). Note the proton–^{7}Li threshold is $E_{th} = 17.2551$ MeV above the ^{8}Be GS. By treating Λ as the high momentum scale, the 1^+ states can be considered as composed of "point" particle ^{7}Li and proton in the EFT framework. Since the ^{8}Be GS is 17.2551 MeV below the proton–^{7}Li threshold and dominated by two ^{4}He cluster configuration [13,14], it can be considered as a deep bound state in terms of the proton–^{7}Li configuration. Therefore, the transitions between the 1^+ states and the ^{8}Be GS happen in short distance as compared to 5 fm. These observations suggest that the reactions can be studied in the EFT framework, in which fields with the corresponding parity and spin are assigned to the involved particles and used to construct interaction operators in the lagrangian satisfying rotational, Galilean, parity, and time reversal invariance. (This approach has been successfully applied to study ^{8}Li and ^{8}B systems [11].) It should be pointed out that near the proton–^{7}Li threshold, the Coulomb interaction between the ^{7}Li and proton in the incoming channels needs the standard nonperturbative treatment, i.e., using the Coulomb wave function instead of the plane wave in the Feynman diagram evaluation [11].

The relevant Lagrangian is collected here:

$$\begin{aligned}\mathcal{L}_0 &= n^{\dagger\sigma}\left(i\partial_t + \frac{\nabla^2}{2M_\text{n}}\right)n_\sigma + c^{\dagger a}\left(i\partial_t + \frac{\nabla^2}{2M_\text{c}}\right)c_a \\ &\quad + \phi^\dagger\left(i\partial_t + \frac{\nabla^2}{2M_\text{n}} + E_{th}\right)\phi \\ &\quad + \psi^{\dagger i}_{(0)}\left(i\partial_t + \frac{\nabla^2}{2M_\text{nc}} - \Delta_{(0)}\right)\psi_{(0)\,i} \\ &\quad + \psi^{\dagger i}_{(1)}\left(i\partial_t + \frac{\nabla^2}{2M_\text{nc}} - \Delta_{(1)}\right)\psi_{(1)i}\,,\end{aligned} \tag{2.2}$$

$$\begin{aligned}\mathcal{L}_P &= h_{0^3P_1}\psi^{\dagger i}_{(0)}T_i^{kj}\,T_k^{a\sigma}\,c_a V_j n_\sigma + h_{0^5P_1}\psi^{\dagger i}_{(0)}T_i^{\alpha j}\,T_\alpha^{a\sigma}\,c_a V_j n_\sigma \\ &\quad + h_{1^3P_1}\psi^{\dagger i}_{(1)}T_i^{kj}\,T_k^{a\sigma}\,c_a V_j n_\sigma \\ &\quad + h_{1^5P_1}\psi^{\dagger i}_{(1)}T_i^{\alpha j}\,T_\alpha^{a\sigma}\,c_a V_j n_\sigma\,,\end{aligned} \tag{2.3}$$

$$\mathcal{L}_{M1} = d_{M1(0)}\phi^\dagger\mathcal{B}^i\psi_{(0)i} + d_{M1(1)}\phi^\dagger\mathcal{B}^i\psi_{(1)i}\,, \tag{2.4}$$

$$\mathcal{L}_{E1} = -id_{E1}\phi^\dagger\mathcal{E}^i\,T_i^{a\sigma}\,c_a n_\sigma + i\frac{d'_{E1}}{V_\Lambda^2}\phi^\dagger\mathcal{E}^i\,T_i^{a\sigma}\,c_a\boldsymbol{V}^2 n_\sigma\,, \tag{2.5}$$

$$\begin{aligned}\mathcal{L}_{E2} &= d_{E2,1}\phi^\dagger\left(\partial^j\mathcal{E}^i\right)T_{ij}^\alpha\,T_\alpha^{lk}\,T_l^{a\sigma}\,c_a V_k n_\sigma \\ &\quad + d_{E2,2}\phi^\dagger\left(\partial^j\mathcal{E}^i\right)T_{ij}^\alpha\,T_\alpha^{\beta k}\,T_\beta^{a\sigma}\,c_a V_k n_\sigma\,.\end{aligned} \tag{2.6}$$

The complex conjugation of the interaction terms are not explicitly shown. In the fields, n_σ (proton), c_a (^{7}Li), ϕ (^{8}Be GS), $\psi_{(0)i}$ (the MIS 1^+ resonance), $\psi_{(1)i}$ (the MIV 1^+ resonance), the indices